Zn/Co ZIF family: MW synthesis, characterization and stability upon halogen sorption

V. Butova, V. A. Polyakov, A. P. Budnyk, A. M. Aboraia, E. A Bulanova, A. A. Guda; E. A. Reshetnikova, Y. Podkovyrina, C. Lamberti; A. V. Soldatov,

Zn/Co ZIF family: MW synthesis, characterization and stability upon halogen sorption

Polyhedron, **154** (2018) 457-464.
Doi: 10.1016/j.poly.2018.08.006

Doi: 10.1016/j.poly.2018.08.006

Zn/Co ZIF family: MW synthesis, characterization and stability upon halogen sorption

Vera V. Butova[1], Vladimir A. Polyakov[1], Andriy P. Budnyk[1], Abdelaziz M. Aboraia[1,2], Elena A. Bulanova[1], Alexander A. Guda[1], Elena A. Reshetnikova[3], Yulia S. Podkovyrina[1], Carlo Lamberti[1,4], and Alexander V. Soldatov[1]

[1] *The Smart Materials Research Institute, Southern Federal University, 5 Zorge Street, Rostov-on-Don, 344090, Russia*
[2] *Department of Physics, Faculty of Science, Al-Azhar University, 71542 Assiut, Egypt*
[3] *Department of Chemistry, Southern Federal University, 7 Zorge Street, Rostov-on-Don, 344090, Russia*
[4] *Department of Physics, INSTM Reference Center and CrisDi and NIS Interdepartmental Centers, University of Turin, Via P. Giuria 1, 10125 Turin Italy.*

ABSTRACT

The bimetallic Zn/Co-ZIF MOFs with different Zn:Co ratio were produced by microwave-assisted solvothermal synthesis. The morphological, structural and electronic properties of the obtained materials were probed with different experimental techniques (XRD, TEM, TGA, BET, UV-Vis, IR, Co and Zn K-edge XANES. The result of the overall characterization study evidences that: (i) for all Zn:Co ratio Zn/Co-ZIFs are isostructural to ZIF-8; (ii) Zn and Co occupy the same crystallographic site having the same local environment; (iii) increasing Co content results in the decrease of solvent and iodine amount adsorbed on the surface of the crystals, while the amount adsorbed inside the pores is almost constant. The Zn/Co-ZIF MOFs were tested for iodine and chlorine sorption.

Keywords: MOF, microwave synthesis, ZIF-8, ZIF-67, bimetallic, iodine adsorption, iodine capping

1. Introduction

Metal-organic frameworks (MOFs) are relatively new porous materials that have already found applications in several different areas such as gas: storage, separation, sensors, catalysis [1-20]. MOFs have a modular structure that can be divided into inorganic clusters with metal ions, and organic linkers coordinating them into a 3-dimentional crystal framework [21]. The type of inorganic cluster and linkers strongly influences the topology of the framework, the physicochemical properties of the MOF and, consequently, its efficiency in various applications [22-26]. Most MOFs studied over the past decades are based on a single type of metal site and on a single linker [18, 19, 27-38]. In this work we will not discuss MOFs synthesized with different linkers [39-51] while we will focus on MOFs synthesized with different metals in the secondary building unit (SBU). The presence of two or more different metals in the same structure can lead not only to the summation of properties, but to have a synergistic effect [52-58]. For example, the mixture of Zn and Co metals provides the fluorescent properties to $Co_2Zn_5(OH)_8(DTA)_3{\cdot}H_2O_n$ [56]. The Zn-doped structure of $Cu_{3-x}Zn_x(BTC)_2$ (BTC = benzenetricarboxylate) exhibits improved magnetic properties in comparison to the initial Cu_3BTC_2 compound [54]. The most common strategy for obtaining the mixed MOFs is based on the insertion of a second

metal in the primary MOF structure by means of immersion, metal exchange or core-shell methods [59-62]. Direct synthesis of mixed MOF is the most convenient and obvious technique; however, it seems to be still a challenging task since it is difficult to evaluate the mechanism of introduction of the second metal. In some cases, each metal can independently form distinct, mono-metallic, MOF crystals without bounding the SBUs containing the other metal. Alternatively, some examples of post-synthesis functionalization with a second metal of an already formed MOFs are also been reported in the literature [55, 57, 58]. In this regard, the MOFs allowing to obtain a mixture of metals within a single crystal structure, attracts special attention. Such compounds include, in particular, the MOF of the ZIF family (ZIF-zeolitic imidazolate frameworks). Their properties, such as high porosity, thermal (>550° in N_2) and chemical stability, make them attractive in several applications such as gas sorption and storage, separation, catalysis [50, 63-77]. Among many ZIF structures, ZIF-8 is the most studied structure because of its potential application for gas separation and selective iodine adsorption [68, 69, 78-81]. This MOF consists of the Zn^{2+} ions coordinated tetrahedrally by nitrogen from the imidazole ring of the 2-methylimidazole linker (MIm). More recently, it has been found that Zn^{2+} ions in the ZIF-8 lattice can be partially or completely replaced by the Co^{2+} ions, which have the same charge and are close in size, providing materials with new properties. The endmember specimen with only cobalt has been named ZIF-67. At present, various methods for the production of bimetallic Zn/Co-ZIF-8 are described in the literature [82-86].

Kaur et al. [82] described bimetallic Zn/Co-ZIF-8 and noted an increase in the pore volume and active surface area in comparison with the initial ZIF-8. Also, recently, Wang et al. [87] described the realization of Zn/Co-ZIF-8 membranes for propane/propylene separation founding that the selectivity of the membranes to propylene increases with the increase of the Co^{2+}/Zn^{2+} ratio in the bimetallic ZIF structure. It was demonstrated that doping of ZIF-8 by Co^{2+} enhances the photodegradation of methylene blue dye under visible light irradiation without hydrogen peroxide [77]. ZIF-8 shows better performance for I_2 adsorption than ZIF-67, it means that the reactive metal site plays a role in the I_2 adsorption [88]. Electrodeless quartz crystal microbalance was used for investigating the adsorption kinetics of iodine onto ZIF-8 and ZIF-67 films; the study revealed a high iodine capacity for both materials (2.4 g/g - ZIF-8 and 4.4 g/g - ZIF-67) [89-91].

The last two are relevant points, as one of the most remarkable specific applications of ZIF-8 is iodine adsorption [78]. It should be noted, that for the iodine capping during the past decades, a list of materials was applied. Part of them physically adsorbed iodine gas, like activated carbons and graphene [92-94], polymers [95-98], cements [99, 100], zeolites [101, 102], hydrotalcites [103] etc. Other materials were functionalized with active species; this is the case e.g. of silver or bismuth particles or ions in the matrix of alumina [104], silica [105] or zeolites [106, 107], which can chemically interact with iodine. Also a large list of MOFs was tested for this application [108-121]. All these materials have advantages and disadvantages in this specific application; among others ZIF-8 combines high iodine capacity with high temperature of iodine evacuation.

The iodine adsorption is facilitated by the favorable interactions between I_2 and MIm linker. Later report proved that ZIF-8 framework strongly binds iodine molecules, while I_2 located on the surface of ZIF-8 are restrained by traditional iodine−organic complexes [122]. The strong interaction is driven by the ideal geometry of the ZIF-8 cage, allowing

the formation of the two iodine−organic bonds per I_2 molecule. The small pore aperture to the cage combined with strong I_2 - cage binding energy resulted in the retain of iodine up to framework collapse[122]. Comparison of three ZIFs with different linkers (ZIF-4, ZIF-8 and ZIF-69) reported in 2013 proved that ZIF-8 is the best option for sorption and retaining of iodine [123]. Large pore apertures (like in ZIF-69) enhance the iodine uptake but reduce the retaining properties. It was demonstrated that the amortization of the ZIFs using ball-milling or high-pressure significantly increases the temperature at which I_2 is retained [123, 124]. Molecular modeling demonstrates that, at low pressure, MOFs with small pore volumes are more qualified for iodine capture; however, at normal pressure, MOFs with high pore volumes are desired [125]. To enhance iodine sorption properties composite materials could be envisaged. A flexible nanocomposite consisting of bacterial cellulose and ZIF-8 nanoparticles was applied for reversible iodine adsorption both from gas phase and I_2/KI solution [126]. High iodine uptake (1.9 g/g from the vapor and 1.3 g/g from the solution) was demonstrated. Composite materials constructed from thin films of ZIF-8 and a glassy Matrimid or a rubbery polyurethane matrix demonstrated higher iodine affinity resulted in better absorptive and retention capabilities than the single phase ZIF-8 material [127]. Specific adsorption of iodine by ZIF-8 could have additional applications such as: (i) electrical detection of the iodine vapor [128]; antimicrobial action [129].
Examples of bromine and chlorine sorption by MOFs, such as the reversible sorption of Cl_2 and Br_2 by cobalt-based MOF [130], are rare in the literature. In 2016 high bromine vapor capacity for ZIF-8 films grown on the surface of quartz was revealed [131].
In the present work, we report a fast microwave (MW) assisted synthesis technique allowing to obtain bimetallic Co^{2+}/Zn^{2+} ZIFs with ZIF-8 structure type. Moreover, comprehensive characterization of the obtained materials is provided. Obtained ZIFs were successfully applied for iodine sorption. Interaction of ZIFs with aggressive chlorine gas was performed too.

2. Experimental details

2.1. Reagents and characterization methods

Reagents $Zn(NO_3)_2 \cdot 6H_2O$, $Co(NO_3)_2 \cdot 6H_2O$, triethylamine (TEA) and dimethylformamide (DMF) were purchased from Sigma-Aldrich. Ultra-pure water (18 MΩ·cm) was produced by SimplicityUV (Millipore) from distilled water.
Laboratory MW system Mars6 (CEM) was employed for the synthesis. Powder X-ray diffraction (PXRD) of samples were collected using D2 Phaser (Bruker) X-ray diffractometer with Cu Kα radiation. The Fullprof program was used for the Rietveld refinement of the diffraction patterns of the as-prepared samples. Diffuse reflectance (DR) UV–Vis spectra were collected on UV-2600 (Shimadzu) spectrophotometer with 2 nm step by using integrating sphere accessory with $BaSO_4$ blank. The measured %R values were converted into absorbance on instrument's software. Transmission electron microscopy (TEM) was performed on FEI Tecnai G2 Spirit TWIN transmission electron microscope operated at an accelerating voltage of 80 kV. Particle size distribution histogram was build based on graphical analysis of 100 NPs in ImageJ software. The experimental XANES spectra of Co *K*-edge (7709 eV) and Zn *K*-edge (9659 eV) were measured for $Zn_{1-x}Co_xC_8H_{10}N_4$ samples using in-house X-ray spectrometer Rigaku R-XAS Looper. A tungsten cathode and a Ge (311) crystal monochromator were used. X-ray tube voltage was

20 kV and current was 70 mA during Co *K*-edge measurements, while for Zn *K*-edge measurements voltage were reduced down to 11 kV. A gas-filled proportional counter (argon gas at a pressure of 300 mbar) was used to register the intensity of the incident radiation, while a scintillation detector was used to register transmitted radiation.

2.2. Synthesis of bimetallic Zn/Co-ZIF

The bimetallic Zn/Co-ZIFs were synthesized according to the previously reported technique [132]. Briefly, zinc and cobalt nitrates hexahydrates and 2-methilimidazole were dissolved separately in the equal volumes of DMF. Then TEA was added to the linker and both solutions were transferred into the glass vessel, closed hermetically and placed into the MW oven (see

Table ***1***). Then reaction mixture was heated at 140 °C for 15 min. After cooling down to room temperature, a precipitate was collected by centrifugation, washed two times with DMF and once with methanol and dried at 60 °C overnight (photos of obtained powders are provided in the SI – Fig. S1).

Table 1. Molar ratio of the initial substances and the labels for the Zn/Co-ZIF samples.

Sample designation	Sample formula	Molar ratio				
		Zn	Co	MIm	TEA	DMF
100Zn0Co	$ZnC_8H_{10}N_4$	1	0	4	2.6	289
95Zn5Co	$Zn_{0.95}Co_{0.05}C_8H_{10}N_4$	0.95	0.05	4	2.6	289
75Zn25Co	$Zn_{0.75}Co_{0.25}C_8H_{10}N_4$	0.75	0.25	4	2.6	289
50Zn50Co	$Zn_{0.5}Co_{0.5}C_8H_{10}N_4$	0.5	0.5	4	2.6	289
0Zn100Co	$CoC_8H_{10}N_4$	0	1	4	2.6	289

2.3. Iodine and Chlorine sorption tests

For Iodine adsorption experiments the respective Zn/Co-ZIF sample was pressed into a thin tablet of about 25-50 mg. The tablet was placed in a glass vessel filled with iodine crystals. The glass vessel was tightly closed and heated up to 110 °C. After iodine full sublimation the sample was held in the iodine atmosphere for 1 h. Finally, the vessel was gently opened to release an excess of iodine (Figure S2). The resulting samples were designated as 100Zn0Co-I, 95Zn5Co-I, 75Zn25Co-I, 50Zn50Co-I, and 0Zn100Co-I.

For Chlorine adsorption experiment we used three initial Zn/Co-ZIF samples: 100Zn0Co, 50Zn50Co, 0Zn100Co. Chlorine gas was obtained by the reaction of HCl acid with $KMnO_4$ (Figure S3). Each sample was treated with the Cl_2 gas at room temperature for 50 min. These samples were designated as 100Zn0Co-Cl, 50Zn50Co-Cl, 0Zn100Co-Cl.

Although, we did not experience any problems in performing the tests, care must be taken while operating with halogens.

3. Results and discussion

3.1. *Bimetallic Zn/Co-ZIF*

The powder XRD patterns are shown in Figure 1. All samples are highly crystalline and isostructural to ZIF-8. No crystalline impurities are detected in the Rietveld refinement (see Fig. S4 and Table S1 for details), and all reflections can be indexed using the cubic space group (I -4 3 m). The correspondent FTIR spectra (Fig. S5) match well too, evidencing

chemical purity of the samples. Both XRD and FTIR data are in a good agreement with reported by other groups [77, 133].

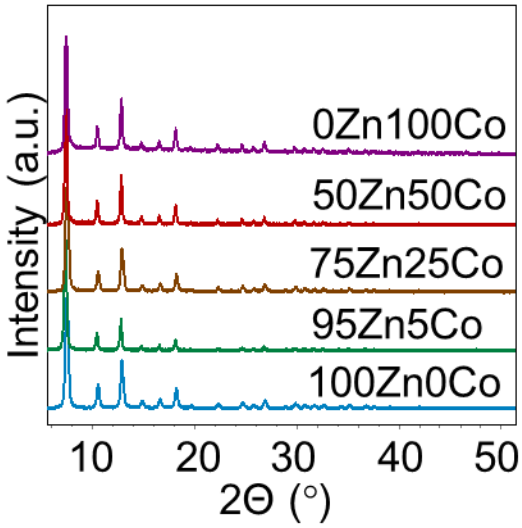

Figure 1. XRD patterns of the synthesized Zn/Co-ZIF samples. See Table 1 for designation.

Thermal stability was investigated by a combination of TGA and XRD techniques (Figure 2 and Fig. S6). It was observed that sample 0Zn100Co have slightly lower temperature of decomposition in the air – about 350 °C, while all other compounds were stable upon the heating up to 400 °C. The products of decomposition are ZnO for 100Zn0Co sample, Co_3O_4 for 0Zn100Co sample and their mixture for the 50Zn50Co sample. The TGA curves of the samples with high zinc content had greater first weight loss associated with the amount of adsorbed solvent (Figure S7).

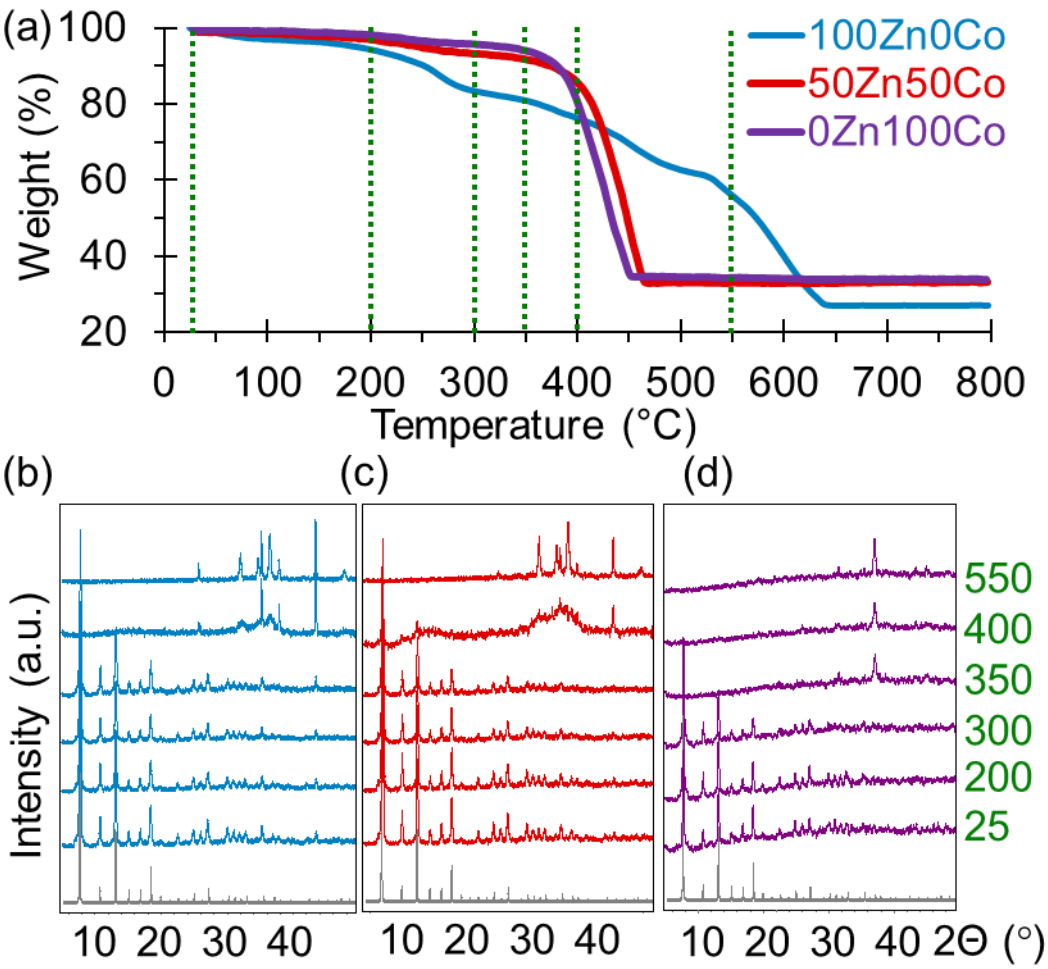

Figure 2 (a) TGA curves of the 100Zn0Co, 50Zn50Co and 0Zn100Co samples measured in air flow. Vertical dotted lines represent selected temperatures used for XRD measurements. (b), (c), (d) XRD profiles obtained in the high temperature chamber at different temperatures (provided in the right part of figure) for samples 100Zn0Co, 50Zn50C0 and 0Zn100Co, respectively.

As all samples were treated identically after synthesis, we suppose that this solvent is absorbed by the surface of the crystals during the sample preparation before measurements. This fact is in good agreement with the nitrogen adsorption measurements (Figure 3). As it could be observed, isotherm of the 100Zn0Co sample has large hysteresis loop at high relative pressure region, while the adsorption/desorption branches of the 0Zn100Co isotherm are almost merged. This indicates a second porosity on the external surface of the samples with high zinc content [134] in good agreement with external surface area, calculated from the nitrogen adsorption data (Table 2). Moreover, the same effect could be attributed to the decrease of structure flexibility with increase of cobalt content due to higher stiffness of Co-N bonds in comparison with Zn-N ones [83, 135]. The specific surface areas of the obtained samples are consistent with each other (Table 2). The N_2 adsorption isotherms are all of type-I suggesting the microporous nature for the samples (Figure S8).

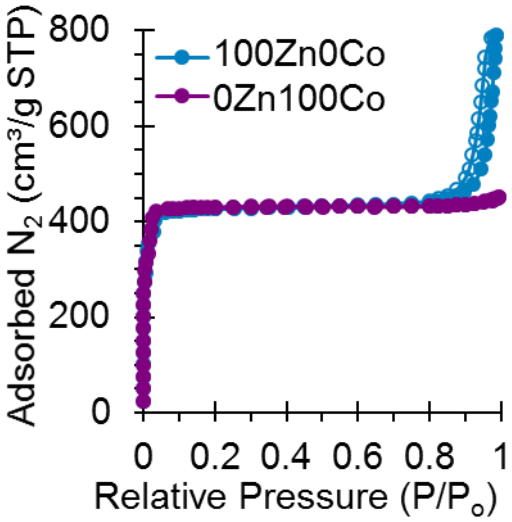

Figure 3 N_2 adsorption – desorption isotherms of the samples 100Zn0Co and 0Zn100Co. Filled markers represents adsorption branches of isotherms, while opened ones – desorption.

The totally random Zn/Co distribution in the sample 75Zn25Co was determined by the SEM-EDS mapping (Figures S9-10, Table S2). The Zn/Co ratio in the synthesized samples was measured by XRF method (Table 2). Slightly lower cobalt content than it was expected from the initial masses of zinc and cobalt salts could be assigned to the stronger interaction between Zn^{2+} and MIm than that between Co^{2+} and MIm [136]. Moreover it was reported that incorporation of Zn^{2+} ions is thermodynamically more favored than that of Co^{2+} in the ZIF structure [77].

Table 2 Surface areas and XRF data for obtained ZIF samples

Sample designation	Specific surface area, m^2/g		t-Plot External Surface Area, m^2/g	Molar ratio (XRF)	
	BET	Langmuir		Zn	Co
100Zn0Co	1553	1871	27.2	-	-
95Zn5Co	1479	1781	18.8	96.8	3.2
75Zn25Co	1523	1835	21.3	78.5	21.5
50Zn50Co	1528	1840	8.4	55.0	45.0
0Zn100Co	1567	1887	4.0	-	-

TEM images of all samples revealed hexagonal crystals with the diameter ranged from 35.07 to 59.4 nm. Data for samples 100ZnoCo, 50Zn50Co and 0Zn100Co is provided in the Figure 4 and for the all other samples with the particle size distribution in the Figure S11.

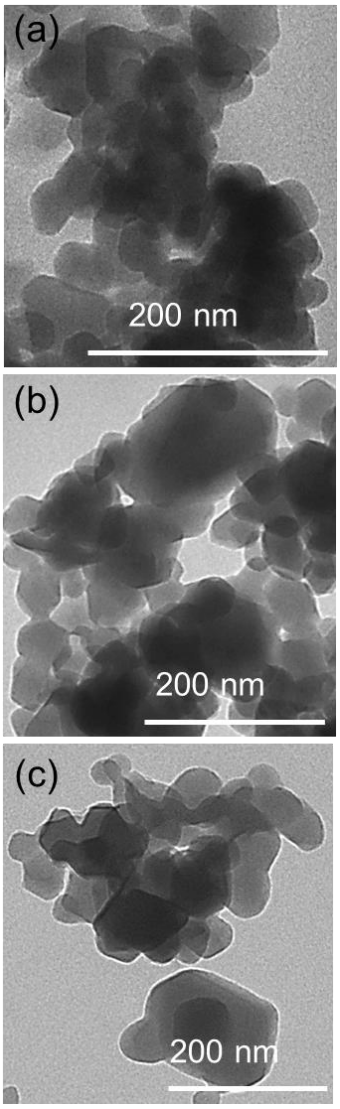

Figure 4 TEM image of the samples 100ZnoCo (a), 50Zn50Co (b) and 0Zn100Co (c).

The optical properties of $Zn_{1-x}Co_xC_8H_{10}N_4$ play an important role for practical applications. UV-vis spectra were measured in the diffuse reflectance mode using Shimadzu UV-2600 spectrophotometer. Absorption as a function of incident wavelength for the series of $Zn_{1-x}Co_xC_8H_{10}N_4$ powder samples are shown in Figure 5 and figure S12. The $Zn_{1-x}Co_xC_8H_{10}N_4$ reveals an UV-vis absorption with three well separated bands at 200, 570 and 1200 nm. Absorption peak at 200 nm corresponds to the $\pi \rightarrow \pi^*$ transition of the aromatic sp^2 domains, as pointed out previously [137]. Intensity of this feature decreases upon increased Co ratio. Two wider and weaker adsorption peaks were observed at 308 and 359 nm. which might arise from the trapping of the excited state energy of the surface states, which can lead to strong fluorescence, as suggested by Chen *et al*. [138].

While for the pure ZIF-8 the only absorption band is located in the UV region cobalt-doped samples show two additional absorption bands. The first, structured absorption band centered at 580 nm with clear three components is due to d-d transition ($^4A_2 \rightarrow {}^4T_1(P)$) of the tetrahedral cobalt(II) ions [139-141]. The second d-d band is found

in the near-infrared region at 1125 nm from $^4A_2 \rightarrow {}^4T_1(F)$ transition. Inspection of the former band shows decrease of intensity of 'middle' component and slight shifting to longer wavelengths of the maximum of this transition with increasing concentration of cobalt(II) ions. A probable explanation for these observations is connected with the decrease of relative amount of surface cobalt(II) ions with increasing size of nanoparticles.

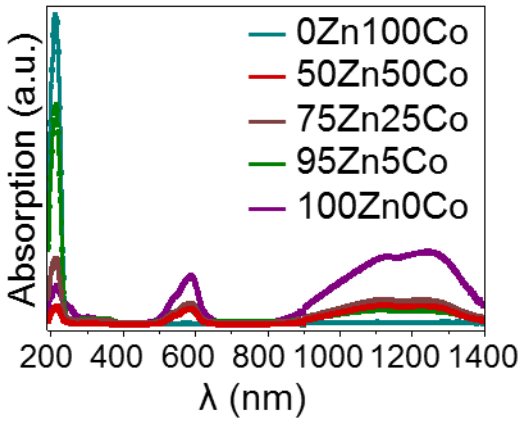

Figure 5 UV-vis absorption spectrum of the $Zn_{1-x}Co_xC_8H_{10}N_4$ nano-powders

X-ray absorption near edge spectroscopy (XANES) is element-specific and local bonding-sensitive technique, which provide information on oxidation state and near-neighbours surrounding of absorption atoms. Figure 6 (a, b) shows that the experimental XANES spectra measured for 95Zn5Co, 75Zn25Co and Z50Zn50Co have common features in comparison with the spectra of initial ZIF structures. This fact allows us to conclude that the local environment around Zn and Co atoms in the structure of bimetallic ZIFs is similar to the structure of monometallic 0Zn100Co and 100Zn0Co. There are not observed chemical shifts between position of white lines of Co *K*-edge and Zn *K*-edge XANES spectra, so it means that $Zn_{1-x}Co_xC_8H_{10}N_4$ samples contain divalent zinc and cobalt ions.

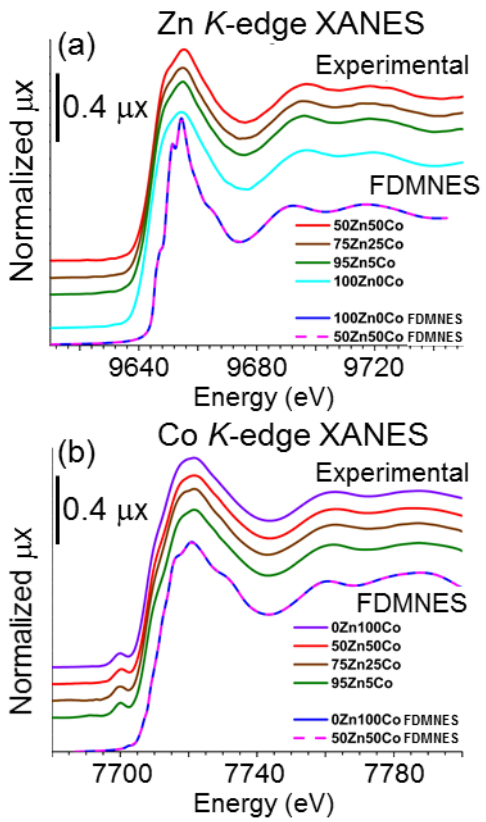

Figure 6 The experimental (a) Zn *K*-edge and (b) Co *K*-edge XANES spectra of $Zn_{1-x}Co_xC_8H_{10}N_4$ samples compared with theoretical spectra, calculated for 0Zn100Co, 100Zn0Co and 50Zn50Co for using FDMNES software

A pre-edge feature (~7,700 eV) on the XANES spectra of the 0Zn100Co and other $Co_{1-x}Co_xC_8H_{10}N_4$ materials (Figure 6b) attributed to 1s→3d electronic transition and clearly indicates that the local environment of cobalt atoms is not centrally symmetric and confirms the tetrahedral symmetry [142, 143]. Accordingly, Cobalt ions in 95Zn5Co, 75Zn25Co and 50Zn50Co samples occupy partially zinc positions with tetrahedral coordination.

XANES spectra reported in Figure 6 (a,b) were simulated using the finite difference method implemented in FDMNES [144] software. To simulate the XANES spectra for 0Zn100Co and 100Zn0Co we used crystallographic data available in Crystallography Open Database. As input geometry we used cluster centered on one of the Zn (for 100Zn0Co) or Co (for 0Zn100Co) atoms with a radius of 6 Å around it. To prove that the local environment of the metal ions in 0Zn100Co and 100Zn0Co does not change after adding another metal to the structure we calculated the XANES spectra for bimetallic 50Zn50Co. For simulations we used the previously described atomic clusters, but metal atom closest to the absorber was substituted by a different one. As it presented in Figure 6 (a, b), theoretical spectra for the monometallic 0Zn100Co and 100Zn0Co structures and bimetallic 50Zn50Co do not have any differences.

3.2. Iodine and chlorine adsorption

XRD and FTIR analysis of the samples after iodine sorption did not revealed any significant changes. (Figure 7, Figure S13-14).

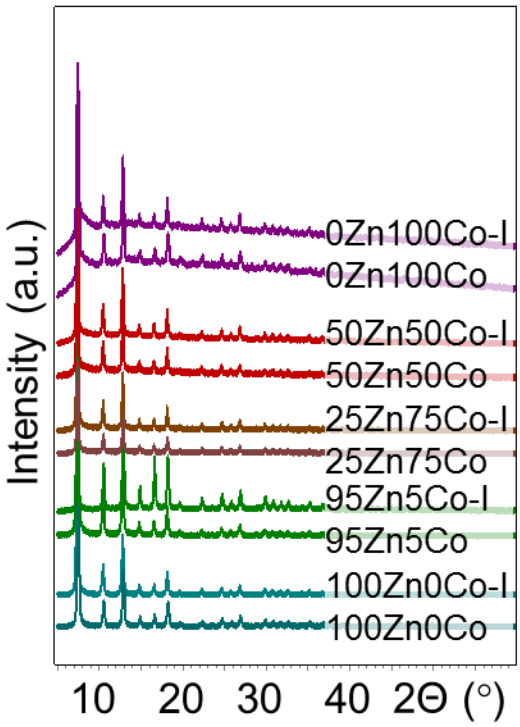

Figure 7 XRD of ZIF samples before and after iodine treatment.

TGA curves of the ZIF samples before and after iodine saturation are presented in the Figure 8 and Figure S15. It could be observed that first low-temperature weight loss (below 350 °C) increased after I_2 treatment. It could be assigned to the iodine molecules, adsorbed on the surface of the crystals. This fact is in good agreement with the increase of a second porosity on the external surface of the initial ZIF samples with the increase of zinc content [134]. Growth of the second weight loss (after 350-400 °C) after iodine saturation could be attributed to the I_2 molecules inside the pores, which could be evacuated only after decomposition of ZIF matrix [78]. This hypothesis is in good agreement with XRF data (Table S3). After iodine treatment the molar ratio I:metal varies from 0.4 up to 1.7 for the different samples and values measured in the different areas of the one sample could varies in wide range. It could be attributed to the sorption of iodine by the external surface of the crystals. After heating at 250 °C the molar ratio I:metal decreases to 0.4-0.6 and values measured in the different areas of the one sample are almost the same. We suppose that after heating iodine molecules from the surface of the crystals were evacuated and the rest of the iodine molecules are located in the pores of the material.

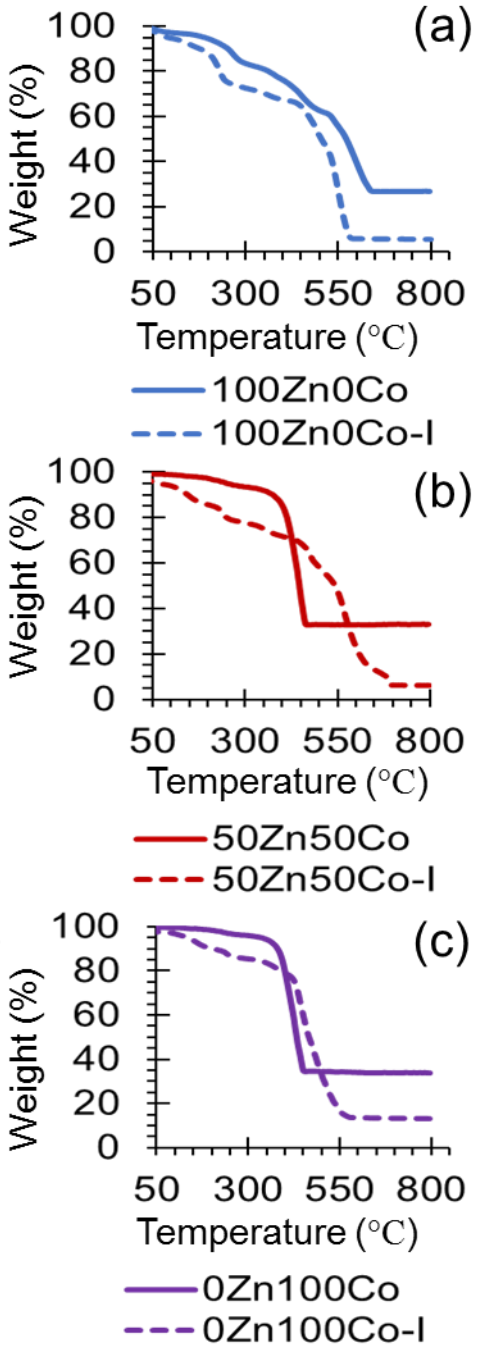

Figure 8 TGA curves of the obtained ZIF samples: 100Zn0Co (a), 50Zn50Co (b) and 0Zn100Co (c) before Iodine treatment (full lines) and after it (dotted lines).

XRD analysis of the ZIF samples after chlorine treatment revealed decomposition of the initial crystal structure (Figure 9).

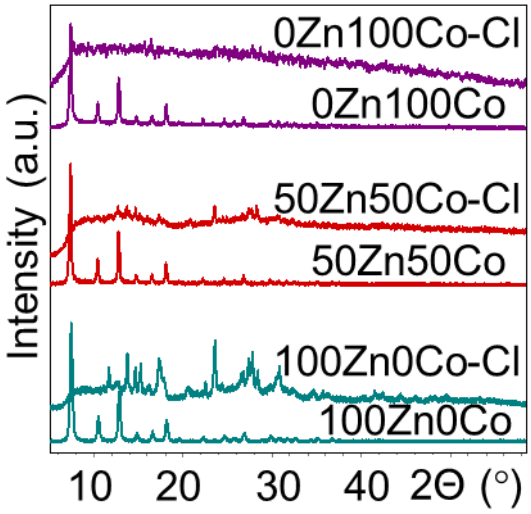

Figure 9 XRD profiles of ZIF samples before and after interaction with Cl_2 gas.

It was also confirmed by spectroscopic investigation. FTIR spectra revealed significant changes in the linker structure. The part of spectra from 600 to 1500 cm^{-1} could be attributed to the vibrations of imidazole ring [133]. It is obvious that the spectrum after chlorine treatment changed (Figure 10). The low-frequency part of spectra demonstrates that modes from Zn-N bonds vanished after chlorine treatment (Figure S16). So we can conclude that after reaction with chlorine gas zinc – linker bonds were distracted, imidazole ring was decomposed. According to FTIR spectra local structure of the amorphous 0Zn100Co-Cl product and crystallin 100Zn0Co product are nearly the same. XRF data revealed close values of chlorine content in respect to metal – about 2:1 (Table S3). Therefore, we can conclude that chlorine treatment results in the decomposition of the linker with formation of the same products independently from the metal content in ZIF.

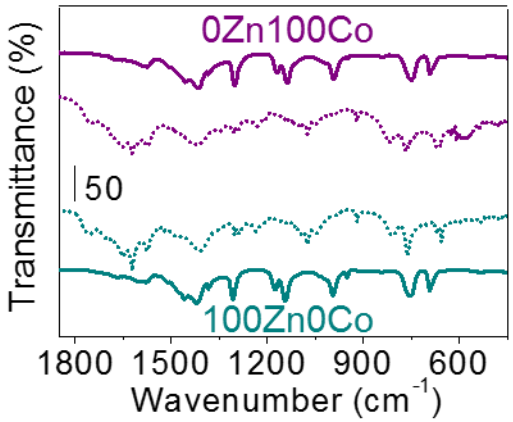

Figure 10 FTIR spectra of samples 100ZnoCo and 0Zn100Co before (full lines) and after (dotted lines) with chlorine gas.

4. Conclusions

Summarizing, MW synthesis technique, which we developed previously for ZIF-8 synthesis [132], could be successfully applied for obtaining ZIF-67 and bimetallic ZIFs with any Zn/Co ratio. Moreover, it allows to synthesize high crystalline samples with

specific surface area about 1500 m^2/g (BET). These samples were comprehensively characterized using wide range of techniques, such as XRD, microscopy, XANES, FTIR. Additionally, stability of obtained samples to halogens was investigated. It was revealed that chlorine initiate decomposition of ZIF structure due to strong oxidizing properties, while iodine could be adsorbed without any significant changes in the crystal structure of ZIF matrix. Cobalt doping decreases external surface of the ZIFs in good agreement with data reported previously [134]. It results in localization of adsorbed iodine molecules inside the pores instead of the surface of the crystals. It could be important for many applications, because I_2 molecules from the surface could be easily removed by heating while iodine from the pores evacuated only with decomposition of ZIF structure (temperature higher than 350 °C).

ACKNOWLEDGMENTS
The research was supported by the Mega-Grant of Ministry of Education and Science of the Russian Federation (14.Y26.31.0001). V.V.B., EAB, and Y.S.P. acknowledge RFBR (research project № 18-33-00584) for financial support.

References

[1] H. Kwak, S.H. Lee, S.H. Kim, Y.M. Lee, B.K. Park, E.Y. Lee, Y.J. Lee, C. Kim, S.J. Kim, Y. Kim, Polyhedron, 27 (2008) 3484-3492.
[2] J. Lee, O.K. Farha, J. Roberts, K.A. Scheidt, S.T. Nguyen, J.T. Hupp, Chem. Soc. Rev., 38 (2009) 1450-1459.
[3] J.R. Li, R.J. Kuppler, H.C. Zhou, Chem. Soc. Rev., 38 (2009) 1477-1504.
[4] D. Farrusseng, S. Aguado, C. Pinel, Angew. Chem.-Int. Edit., 48 (2009) 7502-7513.
[5] L.Q. Ma, C. Abney, W.B. Lin, Chem. Soc. Rev., 38 (2009) 1248-1256.
[6] D. Farrusseng, Ed., Metal-Organic Frameworks: Applications from Catalysis to Gas Storage, Wiley, Weinheim, 2011.
[7] J.R. Li, J. Sculley, H.C. Zhou, Chem. Rev., 112 (2012) 869-932.
[8] A. Corma, H. Garcia, F.X. Llabres i Xamena, Chem. Rev., 110 (2010) 4606-4655.
[9] M. Yoon, R. Srirambalaji, K. Kim, Chem. Rev., 112 (2012) 1196-1231.
[10] Llabres i Xamena, J. Fransesc and Gascon, Metal Organic Frameworks as Heterogeneous Catalysts, The Royal Society of Chemistry, 2013.
[11] D.J. Xiao, E.D. Bloch, J.A. Mason, W.L. Queen, M.R. Hudson, N. Planas, J. Borycz, A.L. Dzubak, P. Verma, K. Lee, F. Bonino, V. Crocella, J. Yano, S. Bordiga, D.G. Truhlar, L. Gagliardi, C.M. Brown, J.R. Long, Nat. Chem., 6 (2014) 590-595.
[12] V.V. Butova, M.A. Soldatov, A.A. Guda, K.A. Lomachenko, C. Lamberti, Russ. Chem. Rev., 85 (2016) 280-307.
[13] E.S. Gutterod, S. Oien-Odegaard, K. Bossers, A.E. Nieuwelink, M. Manzoli, L. Braglia, A. Lazzarini, E. Borfecchia, S. Ahmadigoltapeh, B. Bouchevreau, B.T. Lonstad-Bleken, R. Henry, C. Lamberti, S. Bordiga, B.M. Weckhuysen, K.P. Lillerud, U. Olsbye, Ind. Eng. Chem. Res., 56 (2017) 13207-13219.
[14] T.W. Murinzi, E. Hosten, G.M. Watkins, Polyhedron, 137 (2017) 188-196.
[15] A.D.S. Barbosa, D. Juliao, D.M. Fernandes, A.F. Peixoto, C. Freire, B. de Castro, C.M. Granadeiro, S.S. Balula, L. Cunha-Silva, Polyhedron, 127 (2017) 464-470.
[16] S. Halder, P. Ghosh, C. Rizzoli, P. Banerjee, P. Roy, Polyhedron, 123 (2017) 217-225.
[17] V.V. Butova, A.P. Budnyk, A.A. Guda, K.A. Lomachenko, A.L. Bugaev, A.V. Soldatov, S.M. Chavan, S. Oien-Odegaard, U. Olsbye, K.P. Lillerud, C. Atzori, S. Bordiga, C. Lamberti, Cryst. Growth Des., 17 (2017) 5422-5431.

[18] S. Smolders, K.A. Lomachenko, B. Bueken, A. Struyf, A.L. Bugaev, C. Atzori, N. Stock, C. Lamberti, M.B.J. Roeffaers, D.E. De Vos, ChemPhysChem, 19 (2018) 373-378.
[19] C.A. Stackhouse, S.Q. Ma, Polyhedron, 145 (2018) 154-165.
[20] Y.Z. Chen, R. Zhang, L. Jiao, H.L. Jiang, Coord. Chem. Rev., 362 (2018) 1-23.
[21] O.M. Yaghi, M. O'Keeffe, N.W. Ockwig, H.K. Chae, M. Eddaoudi, J. Kim, Nature, 423 (2003) 705-714.
[22] Q.J. Zhang, B.H. Li, L. Chen, Inorg. Chem., 52 (2013) 9356-9362.
[23] S. Chaemchuen, K. Zhou, N.A. Kabir, Y. Chen, X.X. Ke, G. Van Tendeloo, F. Verpoort, Microporous Mesoporous Mat., 201 (2015) 277-285.
[24] S. Chaemchuem, Z. Kui, F. Verpoort, Crystengcomm, 18 (2016) 7614-7619.
[25] C. Lamberti, A. Zecchina, E. Groppo, S. Bordiga, Chem. Soc. Rev., 39 (2010) 4951-5001.
[26] E. Borfecchia, L. Braglia, F. Bonino, S. Bordiga, S. Øien, U. Olsbye, K.P. Lillerud, J.A. van Bokhoven, K.A. Lomachenko, A.A. Guda, M.A. Soldatov, C. Lamberti, Probing Structure and Reactivity of Metal Centers in Metal–Organic Frameworks by XAS Techniques, in: Y. Iwasawa, K. Asakura, M. Tada (Eds.) XAFS Techniques for Catalysts, Nanomaterials, and Surfaces, Springer International Publishing, Cham, 2017, pp. 397-430.
[27] M. Eddaoudi, D.B. Moler, H.L. Li, B.L. Chen, T.M. Reineke, M. O'Keeffe, O.M. Yaghi, Accounts Chem. Res., 34 (2001) 319-330.
[28] D.J. Tranchemontagne, J.L. Mendoza-Cortes, M. O'Keeffe, O.M. Yaghi, Chem. Soc. Rev., 38 (2009) 1257-1283.
[29] C. Prestipino, L. Regli, J.G. Vitillo, F. Bonino, A. Damin, C. Lamberti, A. Zecchina, P.L. Solari, K.O. Kongshaug, S. Bordiga, Chem. Mat., 18 (2006) 1337-1346.
[30] F. Bonino, S. Chavan, J.G. Vitillo, E. Groppo, G. Agostini, C. Lamberti, P.D.C. Dietzel, C. Prestipino, S. Bordiga, Chem. Mat., 20 (2008) 4957-4968.
[31] J.H. Cavka, S. Jakobsen, U. Olsbye, N. Guillou, C. Lamberti, S. Bordiga, K.P. Lillerud, J. Am. Chem. Soc., 130 (2008) 13850-13851.
[32] N. Masciocchi, S. Galli, V. Colombo, A. Maspero, G. Palmisano, B. Seyyedi, C. Lamberti, S. Bordiga, J. Am. Chem. Soc., 132 (2010) 7902-7904.
[33] S. Chavan, J.G. Vitillo, M.J. Uddin, F. Bonino, C. Lamberti, E. Groppo, K.P. Lillerud, S. Bordiga, Chem. Mat., 22 (2010) 4602-4611.
[34] L. Valenzano, B. Civalleri, S. Chavan, S. Bordiga, M.H. Nilsen, S. Jakobsen, K.P. Lillerud, C. Lamberti, Chem. Mat., 23 (2011) 1700-1718.
[35] S. Chavan, J.G. Vitillo, D. Gianolio, O. Zavorotynska, B. Civalleri, S. Jakobsen, M.H. Nilsen, L. Valenzano, C. Lamberti, K.P. Lillerud, S. Bordiga, Phys. Chem. Chem. Phys., 14 (2012) 1614-1626.
[36] S. Jakobsen, D. Gianolio, D.S. Wragg, M.H. Nilsen, H. Emerich, S. Bordiga, C. Lamberti, U. Olsbye, M. Tilset, K.P. Lillerud, Phys. Rev. B, 86 (2012) 11.
[37] G.C. Shearer, S. Chavan, J. Ethiraj, J.G. Vitillo, S. Svelle, U. Olsbye, C. Lamberti, S. Bordiga, K.P. Lillerud, Chem. Mat., 26 (2014) 4068-4071.
[38] S. Waitschat, D. Frohlich, H. Reinsch, H. Terraschke, K.A. Lomachenko, C. Lamberti, H. Kummer, T. Helling, M. Baumgartner, S. Henningerb, N. Stock, Dalton Trans., 47 (2018) 1062-1070.
[39] D. Sun, G.G. Luo, N. Zhang, J.H. Chen, R.B. Huang, L.R. Lin, L.S. Zheng, Polyhedron, 28 (2009) 2983-2988.
[40] J.M. Verduzco, H. Chung, C.H. Hu, W. Choe, Inorg. Chem., 48 (2009) 9060-9062.
[41] H.X. Deng, C.J. Doonan, H. Furukawa, R.B. Ferreira, J. Towne, C.B. Knobler, B. Wang, O.M. Yaghi, Science, 327 (2010) 846-850.
[42] T. Lescouet, E. Kockrick, G. Bergeret, M. Pera-Titus, S. Aguado, D. Farrusseng, J. Mater. Chem., 22 (2012) 10287-10293.
[43] J.A. Thompson, C.R. Blad, N.A. Brunelli, M.E. Lydon, R.P. Lively, C.W. Jones, S. Nair, Chem. Mat., 24 (2012) 1930-1936.

[44] X.Y. Xu, J.A. van Bokhoven, M. Ranocchiari, ChemCatChem, 6 (2014) 1887-1891.
[45] S. Oien, D. Wragg, H. Reinsch, S. Svelle, S. Bordiga, C. Lamberti, K.P. Lillerud, Cryst. Growth Des., 14 (2014) 5370-5372.
[46] A. Dhakshinamoorthy, A.M. Asiri, H. Garcia, Catal. Sci. Technol., 6 (2016) 5238-5261.
[47] Y.J. Geng, A.Q. Zhang, K.X. Wu, D.X. Xue, Z.H. Liu, Crystengcomm, 18 (2016) 8358-8361.
[48] Z.F. Wu, B. Tan, Z.H. Deng, Z.L. Xie, J.J. Fu, N.N. Shen, X.Y. Huang, Chem.-Eur. J., 22 (2016) 1334-1339.
[49] S.C. Chen, S.N. Lu, F. Tian, N. Li, H.Y. Qian, A.J. Cui, M.Y. He, Q. Chen, Catal. Commun., 95 (2017) 6-11.
[50] L. Xiang, L.Q. Sheng, C.Q. Wang, L.X. Zhang, Y.C. Pan, Y.S. Li, Adv. Mater., 29 (2017) 8.
[51] L. Li, J.Y. Zou, S.Y. You, K.H. Chen, J.Z. Cui, W.M. Wang, Polyhedron, 141 (2018) 262-266.
[52] K.C. Szeto, K.P. Lillerud, M. Tilset, M. Bjorgen, C. Prestipino, A. Zecchina, C. Lamberti, S. Bordiga, J. Phys. Chem. B, 110 (2006) 21509-21520.
[53] K.C. Szeto, C. Prestipino, C. Lamberti, A. Zecchina, S. Bordiga, M. Bjorgen, M. Tilset, K.P. Lillerud, Chem. Mat., 19 (2007) 211-220.
[54] B. Jee, K. Eisinger, F. Gul-E-Noor, M. Bertmer, M. Hartmann, D. Himsl, A. Poppl, J. Phys. Chem. C, 114 (2010) 16630-16639.
[55] C.K. Brozek, M. Dinca, J. Am. Chem. Soc., 135 (2013) 12886-12891.
[56] G.T. Vuong, M.H. Pham, T.O. Do, Dalton Trans., 42 (2013) 550-557.
[57] C.K. Brozek, M. Dinca, Chem. Soc. Rev., 43 (2014) 5456-5467.
[58] A.W. Stubbs, L. Braglia, E. Borfecchia, R.J. Meyer, Y. Roman-Leshkov, C. Lamberti, M. Dinca, ACS Catal., 8 (2018) 596-601.
[59] M. Lalonde, W. Bury, O. Karagiaridi, Z. Brown, J.T. Hupp, O.K. Farha, J. Mater. Chem. A, 1 (2013) 5453-5468.
[60] M.H. Zeng, B. Wang, X.Y. Wang, W.X. Zhang, X.M. Chen, S. Gao, Inorg. Chem., 45 (2006) 7069-7076.
[61] C. Rosler, A. Aijaz, S. Turner, M. Filippousi, A. Shahabi, W. Xia, G. Van Tendeloo, M. Muhler, R.A. Fischer, Chem.-Eur. J., 22 (2016) 3304-+.
[62] A. Knebel, P. Wulfert-Holzmann, S. Friebe, J. Pavel, I. Strauss, A. Mundstock, F. Steinbach, J. Caro, Chem.-Eur. J., 24 (2018) 5728-5733.
[63] K.S. Park, Z. Ni, A.P. Cote, J.Y. Choi, R.D. Huang, F.J. Uribe-Romo, H.K. Chae, M. O'Keeffe, O.M. Yaghi, Proc. Natl. Acad. Sci. U. S. A., 103 (2006) 10186-10191.
[64] H.L. Jiang, B. Liu, T. Akita, M. Haruta, H. Sakurai, Q. Xu, J. Am. Chem. Soc., 131 (2009) 11302-11303.
[65] G. Lu, J.T. Hupp, J. Am. Chem. Soc., 132 (2010) 7832-7833.
[66] Y.C. Pan, Y.Y. Liu, G.F. Zeng, L. Zhao, Z.P. Lai, Chem. Commun., 47 (2011) 2071-2073.
[67] D. Fairen-Jimenez, S.A. Moggach, M.T. Wharmby, P.A. Wright, S. Parsons, T. Duren, J. Am. Chem. Soc., 133 (2011) 8900-8902.
[68] Y.C. Pan, T. Li, G. Lestari, Z.P. Lai, J. Membr. Sci., 390 (2012) 93-98.
[69] H.T. Kwon, H.K. Jeong, Chem. Commun., 49 (2013) 3854-3856.
[70] J.W. Liu, L.F. Chen, H. Cui, J.Y. Zhang, L. Zhang, C.Y. Su, Chem. Soc. Rev., 43 (2014) 6011-6061.
[71] H.X. Zhong, J. Wang, Y.W. Zhang, W.L. Xu, W. Xing, D. Xu, Y.F. Zhang, X.B. Zhang, Angew. Chem.-Int. Edit., 53 (2014) 14235-14239.
[72] G.W. Zhan, H.C. Zeng, Coord. Chem. Rev., 320 (2016) 181-192.
[73] V.V. Butova, A.P. Budnyk, E.A. Bulanova, C. Lamberti, A.V. Soldatov, Solid State Sci., 69 (2017) 13-21.
[74] Y.B. Huang, J. Liang, X.S. Wang, R. Cao, Chem. Soc. Rev., 46 (2017) 126-157.
[75] S.N. Zhao, X.Z. Song, S.Y. Song, H.J. Zhang, Coord. Chem. Rev., 337 (2017) 80-96.

[76] S. Kempahanumakkagari, K. Vellingiri, A. Deep, E.E. Kwon, N. Bolan, K.H. Kim, Coord. Chem. Rev., 357 (2018) 105-129.
[77] D. Saliba, M. Ammar, M. Rammal, M. Al-Ghoul, M. Hmadeh, J. Am. Chem. Soc., 140 (2018) 1812-1823.
[78] D.F. Sava, M.A. Rodriguez, K.W. Chapman, P.J. Chupas, J.A. Greathouse, P.S. Crozier, T.M. Nenoff, J. Am. Chem. Soc., 133 (2011) 12398-12401.
[79] C. Zhang, R.P. Lively, K. Zhang, J.R. Johnson, O. Karvan, W.J. Koros, J. Phys. Chem. Lett., 3 (2012) 2130-2134.
[80] D.F. Sava, T.J. Garino, T.M. Nenoff, Ind. Eng. Chem. Res., 51 (2012) 614-620.
[81] H.T. Kwon, H.K. Jeong, J. Am. Chem. Soc., 135 (2013) 10763-10768.
[82] G. Kaur, R.K. Rai, D. Tyagi, X. Yao, P.Z. Li, X.C. Yang, Y.L. Zhao, Q. Xu, S.K. Singh, J. Mater. Chem. A, 4 (2016) 14932-14938.
[83] F. Hillman, J.M. Zimmerman, S.M. Paek, M.R.A. Hamid, W.T. Lim, H.K. Jeong, J. Mater. Chem. A, 5 (2017) 6090-6099.
[84] Z.W. Hu, Z.Y. Guo, Z.P. Zhang, M.L. Dou, F. Wang, ACS Appl. Mater. Interfaces, 10 (2018) 12651-12658.
[85] X.D. Chen, K. Shen, J.Y. Chen, B.B. Huang, D.N. Ding, L. Zhang, Y.W. Li, Chem. Eng. J., 330 (2017) 736-745.
[86] W. Cheng, C.L. Chen, Y. Yu, C.G. Li, L. Gao, Z. Shi, Chem. J. Chin. Univ.-Chin., 38 (2017) 1303-1308.
[87] C.Q. Wang, F.Q. Yang, L.Q. Sheng, J. Yu, K.X. Yao, L.X. Zhang, Y.C. Pan, Chem. Commun., 52 (2016) 12578-12581.
[88] Y. Yuan, X.Q. Dong, Y.F. Chen, M.H. Zhang, Phys. Chem. Chem. Phys., 18 (2016) 23246-23256.
[89] Q. Kang, X.L. Zhu, X.L. Ma, L.Q. Kong, W.T. Xu, D.Z. Shen, Sens. Actuator B-Chem., 220 (2015) 472-480.
[90] P. Zhang, L.Q. Kong, H.H. Wang, Q. Kang, D.Z. Shen, Sens. Actuator B-Chem., 238 (2017) 744-753.
[91] D.Z. Shen, T.T. Cai, X.L. Zhu, X.L. Ma, L.Q. Kong, Q. Kang, Chin. Chem. Lett., 26 (2015) 1022-1025.
[92] K. Munakata, S. Kanjo, S. Yamatsuki, A. Koga, D. Ianovski, 40 (2003) 695-697.
[93] S.M. Scott, T. Hu, T.K. Yao, G.Q. Xin, J. Lian, Carbon, 90 (2015) 1-8.
[94] S.U. Nandanwar, K. Coldsnow, V. Utgikar, P. Sabharwall, D.E. Aston, Chem. Eng. J., 306 (2016) 369-381.
[95] H.S. Kim, H.H. Cho, J. Appl. Polym. Sci., 47 (1993) 373-375.
[96] R. Ramani, C. Raganathaiah, Appl. Phys. A-Mater. Sci. Process., 64 (1997) 161-165.
[97] R. Ramani, P. Ramachandra, G. Ramgopal, C. Ranganathaiah, J. Appl. Polym. Sci., 68 (1998) 2077-2085.
[98] J. Gacen, J. Maillo, D. Cayuela, I. Gacen, Afinidad, 65 (2008) 342-349.
[99] M. Toyohara, M. Kaneko, H. Ueda, N. Mitsutsuka, H. Fujihara, T. Murase, N. Saito, J. Nucl. Sci. Technol., 37 (2000) 970-978.
[100] M. Toyohara, M. Kaneko, N. Mitsutsuka, H. Fujihara, N. Saito, T. Murase, J. Nucl. Sci. Technol., 39 (2002) 950-956.
[101] M.K. Song, E.Y. Choi, Y. Kim, K. Seff, J. Phys. Chem. B, 107 (2003) 10709-10714.
[102] M. Chebbi, S. Chibani, J.F. Paul, L. Cantrel, M. Badawi, Microporous Mesoporous Mat., 239 (2017) 111-122.
[103] S.P. Paredes, G. Fetter, P. Bosch, S. Bulbulian, J. Nucl. Mater., 359 (2006) 155-161.
[104] T. Fukasawa, K. Funabashi, Y. Kondo, J. Nucl. Sci. Technol., 31 (1994) 1073-1083.
[105] T. Sakurai, A. Takahashi, Y.E. Ming-lu, T. Kihara, S. Fujine, 34 (1997) 211-216.
[106] K.W. Chapman, P.J. Chupas, T.M. Nenoff, J. Am. Chem. Soc., 132 (2010) 8897-+.
[107] J.H. Yang, J.M. Shin, J.J. Park, G. Il Park, M.S. Yim, J. Nucl. Mater., 457 (2015) 1-8.

[108] M.H. Zeng, Q.X. Wang, Y.X. Tan, S. Hu, H.X. Zhao, L.S. Long, M. Kurmoo, J. Am. Chem. Soc., 132 (2010) 2561-+.
[109] W.W. He, S.L. Li, G.S. Yang, Y.Q. Lan, Z.M. Su, Q. Fu, Chem. Commun., 48 (2012) 10001-10003.
[110] G. Ondrey, Chem. Eng., 119 (2012) 14-14.
[111] Z. Yin, Q.X. Wang, M.H. Zeng, J. Am. Chem. Soc., 134 (2012) 4857-4863.
[112] B.J. Xin, G. Zeng, L. Gao, Y. Li, S.H. Xing, J. Hua, G.H. Li, Z. Shi, S.H. Feng, Dalton Trans., 42 (2013) 7562-7568.
[113] H.M. Zhang, J. Yang, Y.C. He, J.F. Ma, Chem.-Asian J., 8 (2013) 2787-2791.
[114] D.F. Sava, K.W. Chapman, M.A. Rodriguez, J.A. Greathouse, P.S. Crozier, H.Y. Zhao, P.J. Chupas, T.M. Nenoff, Chem. Mat., 25 (2013) 2591-2596.
[115] A.K. Chaudhari, S. Mukherjee, S.S. Nagarkar, B. Joarder, S.K. Ghosh, Crystengcomm, 15 (2013) 9465-9471.
[116] X.L. Hu, F.H. Liu, H.N. Wang, C. Qin, C.Y. Sun, Z.M. Su, F.C. Liu, J. Mater. Chem. A, 2 (2014) 14827-14834.
[117] J. Wang, J.H. Luo, X.L. Luo, J. Zhao, D.S. Li, G.H. Li, Q.S. Huo, Y.L. Liu, Cryst. Growth Des., 15 (2015) 915-920.
[118] G. Mehlana, G. Ramon, S.A. Bourne, Microporous Mesoporous Mat., 231 (2016) 21-30.
[119] R.X. Yao, X. Cui, X.X. Jia, F.Q. Zhang, X.M. Zhang, Inorg. Chem., 55 (2016) 9270-9275.
[120] Y.Q. Hu, M.Q. Li, Y.Y. Wang, T. Zhang, P.Q. Liao, Z.P. Zheng, X.M. Chen, Y.Z. Zheng, Chem.-Eur. J., 23 (2017) 8409-8413.
[121] X.R. Zhang, I. da Silva, H.G.W. Godfrey, S.K. Callear, S.A. Sapchenko, Y.Q. Cheng, I. Vitorica-Yrezabal, M.D. Frogley, G. Cinque, C.C. Tang, C. Giacobbe, C. Dejoie, S. Rudic, A.J. Ramirez-Cuesta, M.A. Denecke, S.H. Yang, M. Schroder, J. Am. Chem. Soc., 139 (2017) 16289-16296.
[122] J.T. Hughes, D.F. Sava, T.M. Nenoff, A. Navrotsky, J. Am. Chem. Soc., 135 (2013) 16256-16259.
[123] T.D. Bennett, P.J. Saines, D.A. Keen, J.C. Tan, A.K. Cheetham, Chem.-Eur. J., 19 (2013) 7049-7055.
[124] K.W. Chapman, D.F. Sava, G.J. Halder, P.J. Chupas, T.M. Nenoff, J. Am. Chem. Soc., 133 (2011) 18583-18585.
[125] B. Assfour, T. Assaad, A. Odeh, Chem. Phys. Lett., 610 (2014) 45-49.
[126] A.N. Au-Duong, C.K. Lee, Cryst. Growth Des., 18 (2018) 356-363.
[127] E.M. Mahdi, A.K. Chaudhuri, J.C. Tan, Mol. Syst. Des. Eng., 1 (2016) 122-131.
[128] L.J. Small, T.M. Nenoff, ACS Appl. Mater. Interfaces, 9 (2017) 44649-44655.
[129] A.N. Au-Duong, C.K. Lee, Mater. Sci. Eng. C-Mater. Biol. Appl., 76 (2017) 477-482.
[130] Y. Tulchinsky, C.H. Hendon, K.A. Lomachenko, E. Borfecchia, B.C. Melot, M.R. Hudson, J.D. Tarver, M.D. Korzynski, A.W. Stubbs, J.J. Kagan, C. Lamberti, C.M. Brown, M. Dinca, J. Am. Chem. Soc., 139 (2017) 5992-5997.
[131] D.Z. Shen, L.Q. Kong, X.L. Ma, X.X. Wang, H.H. Wang, Q. Kang, Int. J. Electrochem. Sci., 11 (2016) 3664-3679.
[132] V.V. Butova, A.P. Budnik, E.A. Bulanova, A.V. Soldatov, Mendeleev Commun., 26 (2016) 43-44.
[133] Y. Hu, H. Kazemian, S. Rohani, Y.N. Huang, Y. Song, Chem. Commun., 47 (2011) 12694-12696.
[134] K. Zhou, B. Mousavi, Z.X. Luo, S. Phatanasri, S. Chaemchuen, F. Verpoort, J. Mater. Chem. A, 5 (2017) 952-957.
[135] P. Krokidas, S. Moncho, E.N. Brothers, M. Castier, I.G. Economou, Phys. Chem. Chem. Phys., 20 (2018) 4879-4892.
[136] J. Tang, R.R. Salunkhe, H.B. Zhang, V. Malgras, T. Ahamad, S.M. Alshehri, N. Kobayashi, S. Tominaka, Y. Ide, J.H. Kim, Y. Yamauchi, Sci Rep, 6 (2016).

[137] H.B. Xu, S.H. Zhou, L.L. Xiao, H.H. Wang, S.Z. Li, Q.H. Yuan, J. Mater. Chem. C, 3 (2015) 291-297.
[138] R.Z. Zhang, W. Chen, Biosens. Bioelectron., 55 (2014) 83-90.
[139] J.K. Zareba, M. Nyk, M. Samoc, Cryst. Growth Des., 16 (2016) 6419-6425.
[140] C.F. Bohren, D.R. Huffman, Absorption and scattering of light by small particles, Wiley-VCH, Weinheim, 1983.
[141] F. Wang, Z.S. Liu, H. Yang, Y.X. Tan, J.A. Zhang, Angew. Chem.-Int. Edit., 50 (2011) 450-453.
[142] F. de Groot, G. Vanko, P. Glatzel, J. Phys.-Condes. Matter, 21 (2009).
[143] J.A. Rodriguez, S. Chaturvedi, J.C. Hanson, A. Albornoz, J.L. Brito, J. Phys. Chem. B, 102 (1998) 1347-1355.
[144] S.A. Guda, A.A. Guda, M.A. Soldatov, K.A. Lomachenko, A.L. Bugaev, C. Lamberti, W. Gawelda, C. Bressler, G. Smolentsev, A.V. Soldatov, Y. Joly, J. Chem. Theory Comput., 11 (2015) 4512-4521.

Graphical abstract

for

Zn/Co ZIF family: MW synthesis, characterization and stability upon halogen sorption

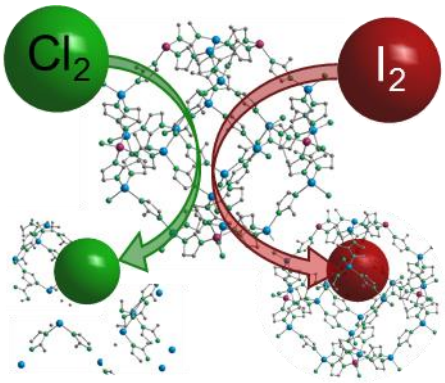

Sinopsys

for

Zn/Co ZIF family: MW synthesis, characterization and stability upon halogen sorption

The bimetallic Zn/Co-ZIF MOFs with different Zn:Co ratio were produced by microwave-assisted solvothermal synthesis. Samples were comprehensively characterized. The Zn/Co-ZIF MOFs were tested for iodine and chlorine sorption.